

DIRECT NUMERICAL SIMULATION OF TURBULENT WAKES: FLOW PAST A SPHERE AT $Re=5000$

I. Rodríguez*, O. Lehmkuhl†, R. Borrell†, A. Oliva‡, C.D. Pèrez-Segarra‡

* Centre Tecnologic de Transferència de Calor (CTTC), Universitat Politècnica de Catalunya
(UPC)
ETSEIAT, Colom 11, 08222, Terrassa, Barcelona, Spain.
e-mail: cttc@cttc.upc.edu

†Termo Fluids, S.L.
Magí Colet, 8, 08204 Sabadell (Barcelona), Spain

‡ Centre Tecnologic de Transferència de Calor (CTTC), Universitat Politècnica de Catalunya
(UPC)
ETSEIAT, Colom 11, 08222, Terrassa, Barcelona, Spain.

Key words: DNS of a sphere, bluff bodies, unstructured grids, turbulence statistics

Abstract. *The flow around bluff bodies is of great interest for a large number of engineering applications such as vehicle aerodynamics, cooling devices using forced convection, heat transfer enhancement using droplets, among others. Although the large number of experimental and numerical studies carried out for the flow past a sphere, there is still lack of detailed information about turbulent statistics in the wake of the sphere. Furthermore, most of the experimental studies consider that the sphere is supported by a stick by its rear side and aligned with the streamwise flow. The objectives of the present work are twofold: i) to carry out the DNS of the flow past a sphere at $Re = 5000$ in order to investigate the characteristics of turbulent flow in the wake of the sphere and provide detailed results of the first and second order turbulent statistics and, ii) to study the influence of the supporting mechanism in the wake configuration as in the turbulence statistics*

1 INTRODUCTION

The flow around bluff bodies is of great interest for a large number of engineering applications such as vehicle aerodynamics, cooling devices using forced convection, heat transfer enhancement using droplets, among others. The unsteady flow over a sphere has been object of many experimental^{1,2,3,4,5} and numerical studies^{6,7,8,9}, most of them providing flow visualization, distribution of the wall skin friction, and integral parameters such as the shedding frequency and the drag coefficient, among others. However, as the three-dimensional and time depending flow behaviour demand the use of fine grids, there is still lack of a complete set of detailed information such as detachment angle, recirculation length and first and second order turbulent statistics in the wake of the sphere at different Reynolds numbers. Such data are not only necessary for validating the results from turbulence modeling but also for testing the behaviour of new models. However, obtaining reliable experimental results implies several difficulties such as finding an adequate supporting mechanism for the sphere and also accurate measurement techniques along the sphere surface and in the near wake.

In addition to the experimental techniques, in the last decades Direct Numerical Simulation (DNS) and Large-Eddy Simulation (LES) have become powerful tools for providing time-accurate useful information about the fluid behaviour. However, one of the major constraints to the simulation of complex turbulent flows is the large amount of computational resources needed to carry them out. By means of the modelisation of some of the turbulence scales (e.g. LES modeling), it is possible to reduce these costs and perform simulations of more complex turbulent flows. In addition, the evolution of parallel computers, that can be commonly formed by thousands of CPU, also allow to multiply the size of the discretisations and the time-integration speed. Therefore, turbulence modeling and developing new efficient algorithms on the parallel architectures available, are both valuable strategies.

Taking advantage of unstructured meshes that allow the use of local grid refinement for accurate solving the flow, without increasing the mesh in the outer zones where laminar regime prevails, we have carried out a DNS of the flow past a sphere at $Re = 5000$. The objectives of work are twofold: i) investigate the characteristics of the turbulent flow in the wake of the sphere and provide detailed information about first and second order turbulence statistics of the flow and, ii) to study the influence of the supporting mechanism in the wake configuration as in the mean flow behaviour. To do this, the computations are performed by using a parallel unstructured symmetry preserving formulation for accurate solving complex geometries. The computational domain simulated is a cylindrical domain of dimensions $[7D, 25D]$ in the (r,z) plane, where D is the sphere diameter located at $(0,5D)$. Considering the geometry of the domain, the mesh used is generated by a constant-step revolution in the azimuthal direction of a two-dimensional (2D) unstructured grid, being $2\pi/N_{planes}$ the step size (N_{planes} is the number of 2D planes in the azimuthal direction). Thus, considering the grid generated by this method, the

Poisson equation that arise from the incompressibility constrain is solved by means of a Fourier diagonalisation method in the periodic direction^{10,11}.

Results are discussed in terms of instantaneous and statistical flow features focussing on the wake structure. Comparison of the present results with those obtained by Seidl et. al.⁶, who investigated the flow around a sphere held by a cylindrical stick, are also presented. Main differences due to geometry are also analysed. The capability of the presented numerical methodology for accurate solving the flow behaviour in complex geometries is also pointed out.

2 MATHEMATICAL AND NUMERICAL MODEL

The Navier-Stokes and continuity equations can be written as

$$\mathbf{M}\mathbf{u} = \mathbf{0} \quad (1)$$

$$\frac{\partial \mathbf{u}}{\partial t} + \mathbf{C}(\mathbf{u})\mathbf{u} + \nu \mathbf{D}\mathbf{u} + \rho^{-1}\mathbf{G}\mathbf{p} = \mathbf{0} \quad (2)$$

where $\mathbf{u} \in \mathbb{R}^{3m}$ and $\mathbf{p} \in \mathbb{R}^m$ are the velocity vector and pressure, respectively (here m applies for the total number of control volumes (CV) of the discretised domain), ν is the kinematic viscosity and ρ the density. Convective and diffusive operators in the momentum equation for the velocity field are given by $\mathbf{C}(\mathbf{u}) = (\mathbf{u} \cdot \nabla) \in \mathbb{R}^{3m \times 3m}$, $\mathbf{D} = \nabla^2 \in \mathbb{R}^{3m \times 3m}$ respectively. Gradient and divergence (of a vector) operators are given by $\mathbf{G} = \nabla \in \mathbb{R}^{3m \times 3m}$ and $\mathbf{M} = \nabla \cdot \in \mathbb{R}^{m \times 3m}$ respectively.

The governing equations have been discretised on a collocated unstructured grid arrangement by means of second-order spectro-consistent schemes (see Verstappen and Veldman¹²). Such schemes are conservative, i.e. they preserve the kinetic-energy equation. These conservation properties are held if and only if the discrete convective operator is skew-symmetric ($\mathbf{C}_c(\mathbf{u}_c) = -\mathbf{C}_c^*(\mathbf{u}_c)$), the negative conjugate transpose of the discrete gradient operator is exactly equal to the divergence operator ($-(\Omega_c \mathbf{G}_c)^* = \mathbf{M}_c$) and the diffusive operator \mathbf{D}_c , is symmetric and positive-definite (the sub-index c holds for the cell-centred discretisation). These properties ensure both, stability and conservation of the kinetic-energy balance even at high Reynolds numbers and with coarse grids.

For the temporal discretisation of the momentum equation (2) a second order backward difference scheme for the time derivative term and, a first-order backward Euler scheme for the pressure gradient term have been used. For the rest of the terms (convective and diffusive) a explicit third-order Gear-like scheme¹³ has been used.

The velocity-pressure coupling has been solved by means of a classical fractional-step projection method,

$$\mathbf{u}_c^p = \mathbf{u}_c^{n+1} + \mathbf{G}\tilde{\mathbf{p}}_c \quad (3)$$

where $\tilde{\mathbf{p}}_c = \mathbf{p}_c^{n+1}\Delta t^n/\rho$ is the pseudo-pressure, \mathbf{u}_c^p the predicted velocity, $n + 1$ is the instant where the temporal variables are calculated, and Δt^n is the current time step

($\Delta t^n = t^{n+1} - t^n$). Taking the divergence of (3) and applying the incompressibility condition yields a discrete Poisson equation for $\tilde{\mathbf{p}}_c$: $\mathbf{L}_c \tilde{\mathbf{p}}_c = \mathbf{M}_c \mathbf{u}_c^p$. The discrete laplacian operator $\mathbf{L}_c \in \mathbb{R}^{m \times m}$ is, by construction, a symmetric positive definite matrix ($\mathbf{L}_c \equiv \mathbf{M}\Omega^{-1}\mathbf{M}^*$). Once the solution of \mathbf{p}_c^{n+1} is obtained, $\tilde{\mathbf{p}}_c$ results from equation 3.

Finally the mass-conserving velocity at the faces ($\mathbf{M}_s \mathbf{u}_s^{n+1} = 0$) is obtained from the correction,

$$\mathbf{u}_s^{n+1} = \mathbf{u}_s^p - \mathbf{G}_s \tilde{\mathbf{p}}_c \quad (4)$$

where \mathbf{G}_s represents the discrete gradient operator at the CV faces. This approximation allows to conserve mass at the faces but it has several implications. If the conservative term is computed using \mathbf{u}_s^{n+1} , in practice an additional term proportional to the third-order derivative of \mathbf{p}_c^{n+1} is introduced. Thus, in many aspects, this approach is similar to the popular Rhie and Chow¹⁴ and eliminates checkerboard modes.

However, collocated meshes do not conserve kinetic energy as have been shown by Morinishi et al.¹⁵ for finite-difference schemes and by Felten and Lund¹⁶ for finite-volume schemes. When the fractional step method is used on a collocated arrangement, there are two sources of errors in the kinetic-energy conservation ϵ_{ke} . These errors are due to: i) interpolation schemes and, ii) inconsistency in the pressure field in order to ensure mass conservation. While the first one can be eliminated through the use of conservative schemes such as those used in the present work, the latter equals to:

$$\epsilon_{\text{ke}} = (\tilde{\mathbf{p}}_c)^* \mathbf{M}_c (\mathbf{G}_c - \mathbf{G}_s) \tilde{\mathbf{p}}_c \quad (5)$$

This contribution of the pressure gradient term to the evolution of the kinetic energy can not be eliminated. Felten and Lund¹⁶ have performed analysis to determine its scaling order. They have shown that the spatial term of the pressure error scales as $\mathcal{O}(\Delta x^2)$ and the temporal term scales as $\mathcal{O}(\Delta t)$, i.e. pressure errors are of the order of $\mathcal{O}(\Delta x^2 \Delta t)$. However, in their work they proved that pressure errors do not have significant impact on the results at grid resolutions and time-steps used in LES and DNS.

3 COMPUTATIONAL ASPECTS

3.1 Geometry discretisation

The mesh used for computations is generated by a constant-step rotation about the axis of a two-dimensional (2D) unstructured grid, being $2\Pi/N_{\text{planes}}$ the step size (N_{planes} is the number of planes in which the azimuthal direction is divided). An example of the grid of the plane and its revolution in the azimuthal direction is shown in Figure 1.

With this kind of mesh, the linear couplings of the discrete Poisson equation in the azimuthal direction are circulant matrices. This allows to solve the Poisson equation by means of a Fourier diagonalisation method^{17,18}. As a result, the initial system is decoupled in N_{planes} 2D mutually independent systems in the resultant spectral space, reducing this way its arithmetical complexity and the RAM memory requirements.

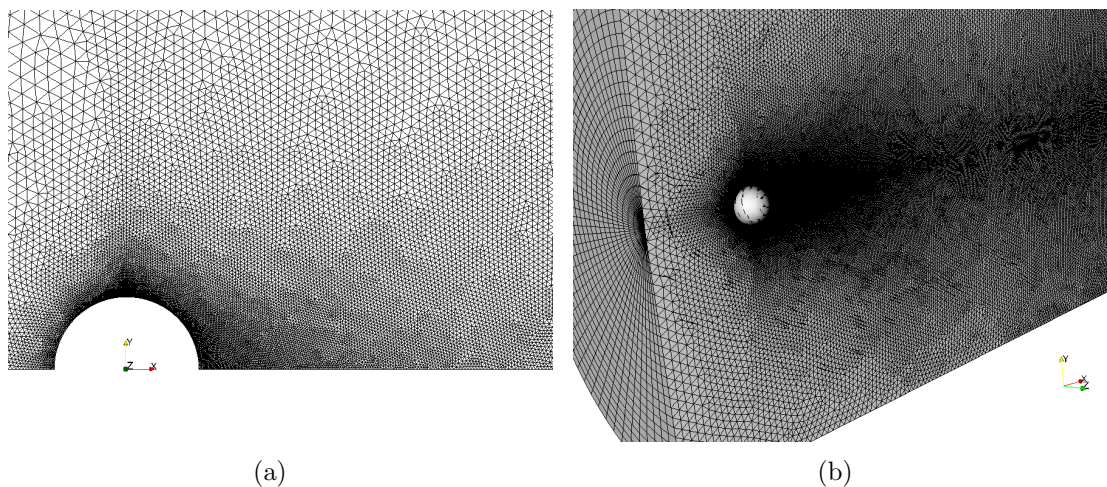


Figure 1: a) Detail of the mesh of the plane in the region near the sphere, b) extruded 3D mesh

The proposed algorithm does not impose any restriction for the original 2D mesh and thus it is suitable for unstructured meshes. Nevertheless, this lack of structure leads to a more complex data management.

3.2 Parallel algorithm for Poisson equation

In the parallel code used to perform the simulations presented in this paper, the algorithm at each time-step is divided into two parts: an implicit part where the Poisson equation is solved to obtain the pressure, and the rest of the calculations that are solved in an explicit manner.

In the explicit part, a point to point communication between each subdomain and its neighbours is needed. The load of this communication depends on the size of the stencils used in the numerical schemes but, in general, it does not significantly degrade the parallelism unless the subdomains are too small. On the contrary, the Poisson equation, which arises from the incompressibility constraint and couples all the nodes of the domain, is usually the main bottleneck from a computational point of view, i.e. in terms of parallelism, RAM memory requirements and CPU-time consumption.

The N_{planes} 2D systems are solved by means of a Schur-based Domain Decomposition method^{19,18,10}. This method is based on the explicit calculation of a Schur complement matrix of the partitioned 2D system, and its direct solution. The main advantages of this direct method are its robustness and its short solution time, as many calculations are made in a pre-process stage. This pre-processing is carried out only once at the beginning of the simulation. Thus, compared to the total integration time its cost is usually negligible.

A simple way to parallelise this linear solver would be distributing the set of N_{planes} 2D systems among the set of available CPUs and solve them independently. However, this is not the best option as for the transformation from physical to spectral space

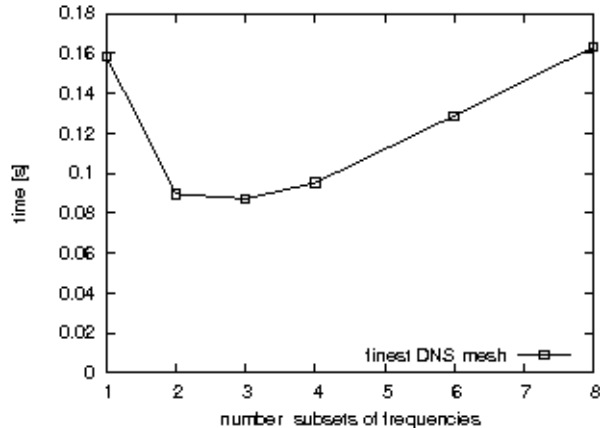


Figure 2: Time spent to solve the Poisson equation with different parallelisation strategies. The size of the mesh of study is 5451552 nodes (56787x96 planes)

(and vice versa), the information of all the frequencies is required. Thus, an all to all communication between all the processors solving different frequency components of the same point is needed. Another option would be using all the CPUs available in the parallelisation of the 2D solver and solve the frequencies one after another. This option would not be the best when the number of CPUs available overcomes the linear speed-up region of the Schur-based Domain Decomposition method. Considering the different options and depending on the case, the best solution is a combination of both.

Figure 2 illustrates the time spent for solving the Poisson equation as a function of the number of subsets of frequencies in which the homogeneous direction is divided for a mesh of 56787×96 planes. In the example, a total number of 96 CPU have been used. In this case, the best option is to divide the azimuthal set of frequencies into 3 subsets and to use 32 CPUs for parallelising the 2D solver. All computations reported in this paper have been performed on a cluster composed of 76 nodes (each node had 2 AMD opteron 2350 Quad Core processors linked in an infiniband DDR4X network).

4 DESCRIPTION OF THE CASE

Numerical simulations of the flow over a sphere have been performed at $Re = 5000$, where Reynolds number ($Re = UD/\nu$) is defined in terms of the free-stream velocity U and the sphere diameter D . Solutions are obtained on a cylindrical computational domain of dimensions $x=[-5D,20D]$; $r=[0,7D]$; $\theta=[0,2\pi]$, where the sphere is located at $(0,0,0)$ (see figure 3). The boundary conditions at the inflow consist of a uniform velocity $(u,v,w)=(1,0,0)$. Constant velocity $(u,v,w)=(1,0,0)$ is also prescribed at the other external boundaries except for the downstream one (outlet) where a pressure-based condition is used. No-slip conditions on the sphere are imposed.

The governing equations are solved on an unstructured mesh generated by the constant-

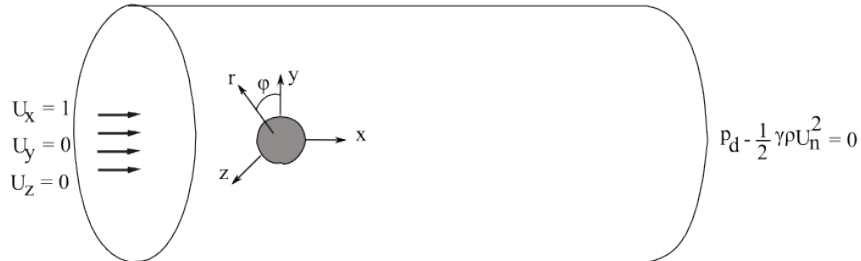


Figure 3: Computational domain and boundary conditions

step rotation around the axis of a two-dimensional unstructured grid in a (x,r) plane. The use of an unstructured grid for the mesh of the plane has allowed to cluster more control volumes around the sphere and in the near wake. The results presented in the present work have been obtained on a grid with about 7.68 MCVs (80054×96 planes). In order to ensure that boundary layer is well resolved about 12 CVs have been placed inside the boundary layer, with the first grid point located at a normal wall distance of $x/D = 7.5 \times 10^{-4}$. For comparison purpose, a coarse grid of about 3.66 MCVs (57131×64 planes) has also been solved.

One of the major difficulties for obtaining reliable experimental results are to find an adequate supporting mechanism for the sphere. Some experimental set-ups use a stick at the rear end of the sphere for holding it, but it might be expected that this support can affect not only the statistical results but also the structure of the wake. Thus, in order to study the influence of the holding support in the wake of the sphere another configuration has been considered. In this case, geometry consists of a sphere of diameter D held by the rear side for a stick of diameter $d = 0.1D$. With the exception of the stick, the geometry considered is the same as described for the primary case. For this configuration, the grid considered is also similar, with about 8.23 MCVs (85729×96 planes).

In order to calculate turbulence statistics, the initially homogeneous flow field has been advanced in time until statistical stationary flow has been established. Then, first and second order statistics are based on the integration of instantaneous data over a period of $140 D/U$ time-units for the sphere without stick. These statistics have been also averaged in the azimuthal direction. For this integration period, the resolved turbulence statistics presented should be considered as statistically converged values. However, for the case of the sphere held by a stick, it has been observed that there is required a larger integration time for turbulent statistics. Thus in the present paper, only instantaneous results for this case are presented.

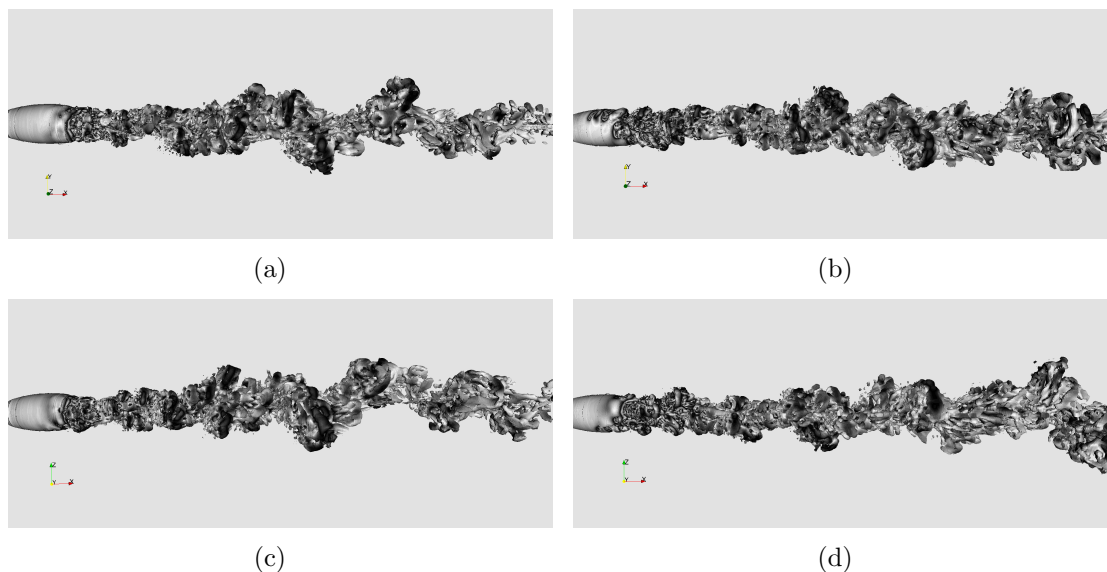


Figure 4: Instantaneous vortical structures in the wake of the sphere by means of Q-iso-surfaces. (a) and (c) sphere without supporting mechanism at two different azimuthal positions. (b) and (d) sphere held by a stick at two different azimuthal positions

5 RESULTS

5.1 Instantaneous flow

Coherent-structures in the near wake have been represented by Q-iso-surfaces (see Hunt et al.²⁰). The Q-criterion proposed by Hunt et al. defines an eddy structure as a region with positive second invariant of the velocity gradient tensor $\nabla\mathbf{u}$. Positive values of Q represents that vorticity prevails over strain, i.e. the strength of rotation overcomes the strain.

A general view of the coherent-structures in the wake represented for the case without the stick (figures 4(a) and 4(c)) and with the stick (figures 4(b) and 4(d)) are shown. In the figure, structures are depicted in two different views, i.e. viewed from different azimuthal positions.

As it is shown in the figures, the fluid separates laminaarly from the sphere. The separation angle is about 89° . This result is in agreement with previous observation of Seidl et al.⁶ for a sphere at $Re = 5000$. The separated shear layer remains laminar until at a certain position some instabilities appear. These instabilities occur at random azimuthal locations causing the vortex-sheet rolling-up, the flow becoming three-dimensional and finally the transition to turbulence. Once the axial symmetry of the shear layer is broken, the vortex formed breaks into small scale vortices in the separated zone and feed the turbulent wake.

There are no great differences in the large-scale flow, but apparently, the first instabilities in the separated shear layer for the case with the sphere support occurs at positions

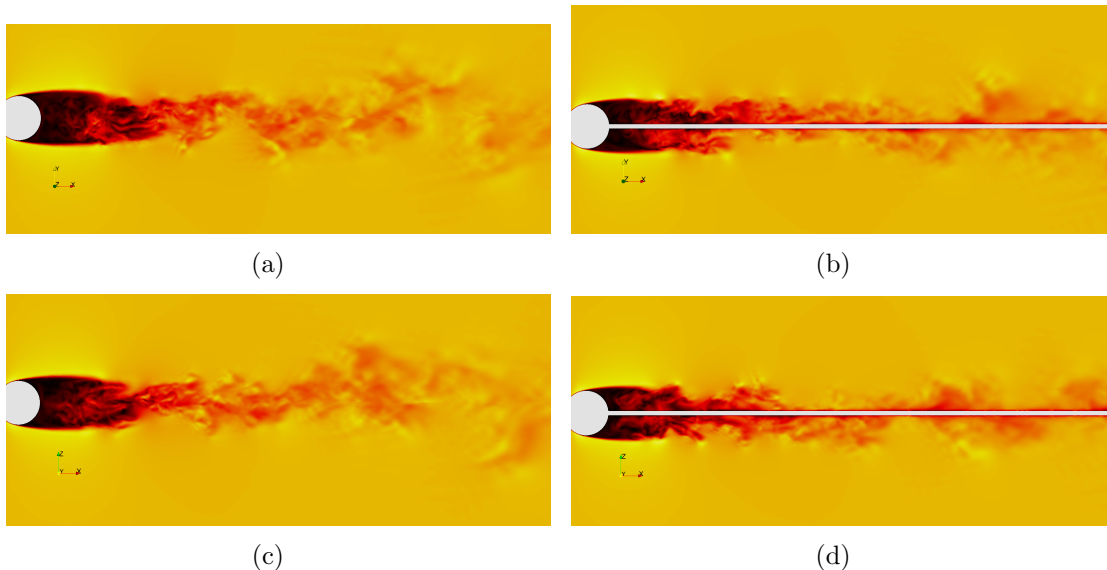


Figure 5: Instantaneous velocity contours in the wake of the sphere. (a) and (c) sphere without supporting mechanism at two perpendicular planes. (b) and (d) sphere held by a stick at two perpendicular planes.

closer to the sphere, than the case without support. In addition, it also can be observed that large-scale waviness is more pronounced in the case without support (figures 4(a) and 4(c)). It seems as if the shedding of vortices in the separated shear layer is affected by the supporting stick and thus, as it breaks somehow the waviness motion in the near wake.

Figure 5 shows instantaneous velocity contours at two perpendicular planes in the wake of the sphere for both cases. As has been commented before, in the figure can also be observed how instabilities in the shear layers appear closer to the sphere in the case with supporting mechanism, and also it can be seen how the recirculation zone is shortened by the effect of the stick. All this aspect would affect the turbulence statistics of the flow, and thus they must be confirmed by the time-average of the flow.

5.2 First and second order statistics

As has been commented in section 4, all statistical results presented here have been obtained for the case without the supporting mechanism. The angular distribution of the mean pressure coefficient is plotted in figure 6. In the figure, the mean pressure coefficient is compared with the experimental data by Kim and Durbin³ at $Re = 4200$. As can be seen, when comparing the DNS results a good agreement within experimental uncertainties is obtained. The angular position of the pressure minimum is well captured, being at $\varphi = 72^\circ$. This value is also comparable with the position of the pressure minimum, $\varphi = 71^\circ$, reported by Seidl et al.⁶ at $Re = 5000$.

A direct comparison of mean flow and fluctuations of the streamwise velocity in the

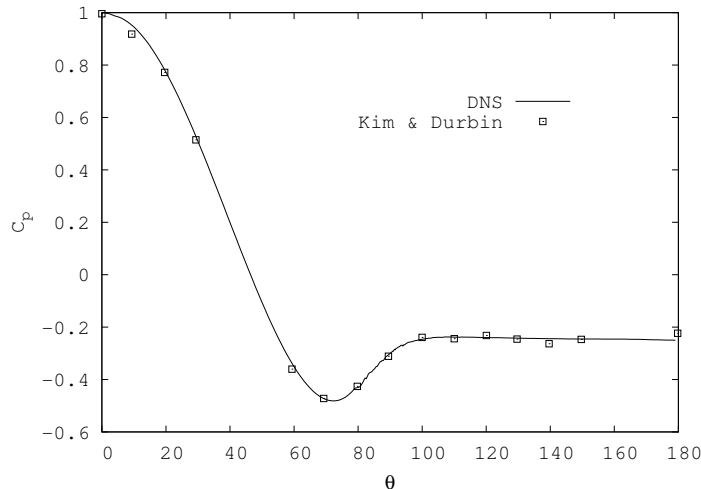


Figure 6: Mean pressure distribution around the sphere compared with experimental results of Kim and Durbin³ at $Re = 4200$.

near wake for the two grids solved are shown in the figures 7 and 8, respectively. Results of the mean streamwise velocity are also compared with the DNS results of Seidl et al.⁶. As can be observed, there is a good agreement between both grids and also with previous DNS for the mean flow quantities. Major discrepancies between both grids are observed in the streamwise velocity fluctuations. These differences are mainly due to the poor resolution of the coarse grid, being not capable of capturing all the scales of the flow.

Some discrepancies are observed with results from Seidl et al⁶ at distances greater than $x/D \geq 2.5$, where according to our DNS results the flow is in the recovery zone (the length of the recirculation bubble is $L = 1.81$), while according with previous DNS⁶ the flow is closer to the end of the recirculation bubble (they reported a recirculation length of $L = 2.1$). These differences might be due to geometric differences or numerics differences. As for the first ones, the previous results⁶ considers a sphere held by a stick, which is still non clear how this support can affect the flow in the wake and thus statistical results. At this point, we have only obtained preliminary results of the influence of the stick, thus further investigation is required about this subject. On the other hand, it has been observed that a long integration time is required for obtaining turbulence statistics. It is probably that differences between the results can be also due to the not so long integration of the statistics on the work reported in the literature (they reported an integration time of only $50D/U$ time units while $140 D/U$ time units are averaged in the present work). In addition, for the case with the sphere held by a stick, we have accumulated more than $85 D/U$ time units since now and we have not observed time independence of the results yet.

In addition to the results for the streamwise first and second order statistics, time-average of the radial velocity and its fluctuations at different locations in the wake of the

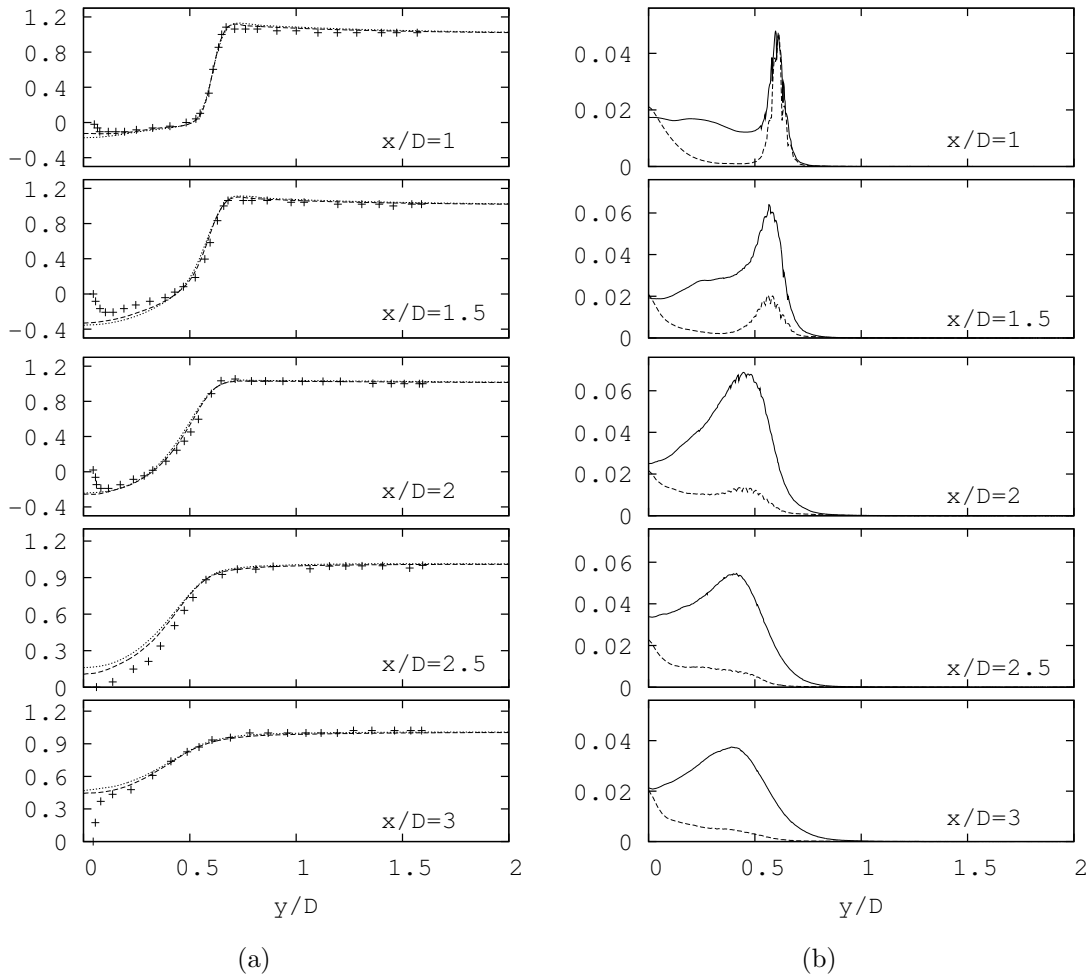


Figure 7: First and second order statistics of the streamwise velocity at different positions in the wake. Solid lines DNS, dashed line coarse DNS, dots DNS by Seidl et al⁶ (a) Streamwise velocity, (b) Fluctuations $\overline{u'u'}/U^2$

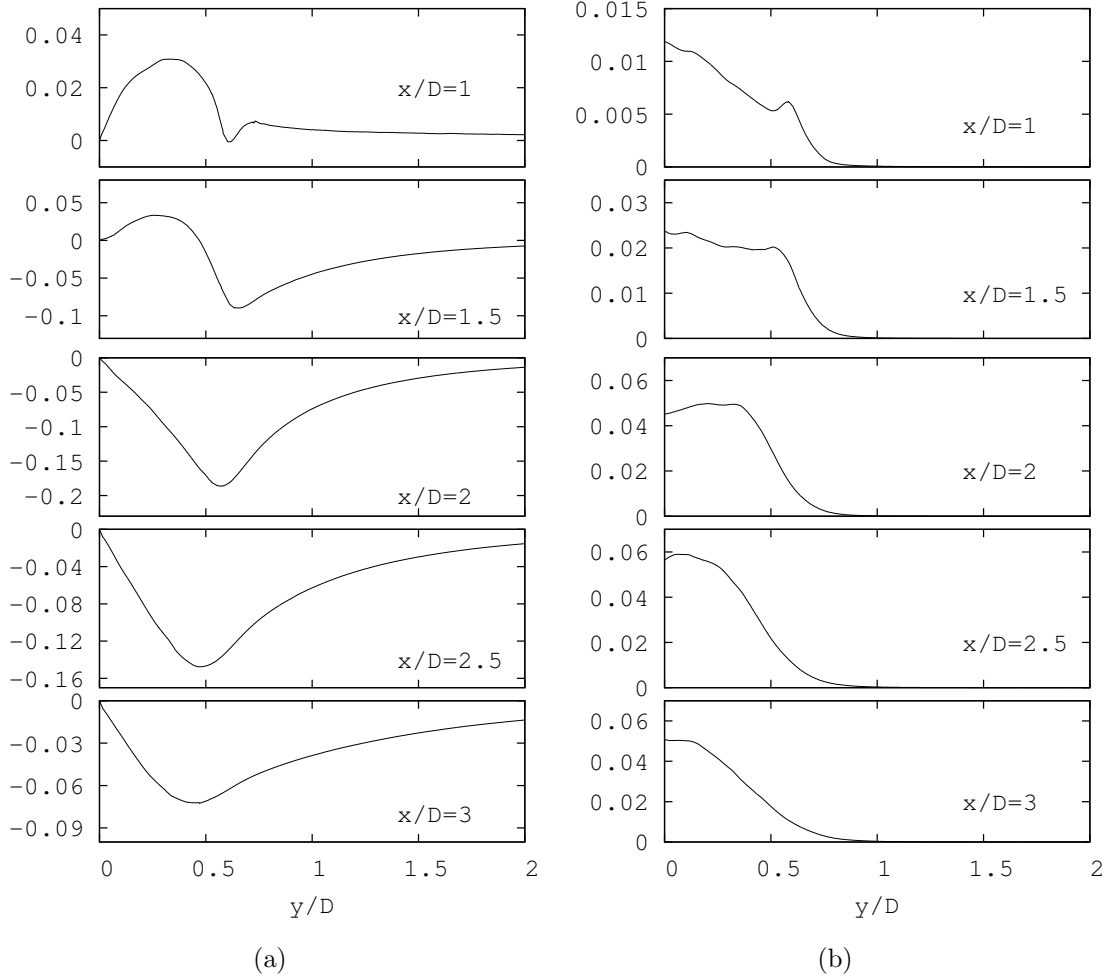


Figure 8: First and second order statistics of the radial velocity at different positions in the wake. (a) radial velocity, (b) Fluctuations $\overline{v'_r v'_r} / U^2$

sphere are given in figure 8.

5.3 Influence of the sphere support. Work on progress

As has been commented previously, it is interesting to analyse the influence of the supporting mechanism for the sphere, used in most of the experimental set-ups. As has been shown, the instantaneous flow seems to be affected by the geometry of the wake, and thus, it is expected that this can be reflected also in the turbulence statistics of the flow.

It was reported previously by Norman and McKeon²¹ in an experimental study carried out with different stick diameters, that the supporting stick does not change significantly the mean wake, but that the Reynolds stresses decrease with the increase of the stick

diameter. However, the quantitative impact of the supporting stick on the statistics of the wake is still unclear.

Up-to-now, we are currently carrying out DNS of the sphere held by a stick of diameter $d = 0.1D$, but average statistics of the flow takes long time to converge, thus more time is still required before we can draw conclusions of the mean flow behaviour.

6 CONCLUSIONS

The DNS of the flow past a sphere at $Re = 5000$ has been carried out. The governing equations have been discretised by means a collocated second-order spectro-consistent formulation that ensures good stability and conservation of the kinetic-energy balance. The results have been computed on a grid of about 7.68 MCVs. In addition to this study, the influence of the supporting mechanism of the sphere is under consideration by carrying out DNS of this geometry on a grid of about 8.23 MCVs.

A large set of first and second order statistics at different positions in the wake for the case without supporting stick is given. As far as the author knowledge is concerned, there were no previous results in the literature providing turbulence statistics for this flow at $Re = 5000$. The presented results constitute an useful data for assessing and validating the results from turbulence modeling.

Moreover, first results analysed have shown that the supporting stick seems to be some influence in the instantaneous flow, causing an earlier transition to turbulence in the shear layer and also provoking the shorten of the recirculation zone. These results are only preliminary and further investigation of the turbulence statistics is required.

It is worth to highlight that the methodology developed for solving bodies of revolutions using unstructured grids has allowed to solve accurately the flow in the wake of the sphere with good results. Furthermore, the computational cost of the present computations is relatively small for the computational grids used, which is encouraging for carrying out DNS at higher Reynolds numbers with a reasonable cost of CPU time and computational resources.

ACKNOWLEDGEMENTS

This work has been by financially supported by the Ministerio de Educación y Ciencia, Secretaría de Estado de Universidades e Investigación, Spain (ref. ENE2009-07689) and by the Collaboration Project between Universidad Politècnica de Catalunya and Termo Fluids S.L. (ref. C06650)

References

- [1] E. Achenbach. Experiments on the flow past spheres at very high Reynolds numbers. *Journal of Fluid Mechanics*, 54:565–575, 1972.
- [2] E. Achenbach. Vortex shedding from spheres. *Journal of Fluid Mechanics*, 62(2):209–221, 1974.

- [3] H.J. Kim and P.A. Durbin. Observations of the frequencies in a sphere wake and of drag increase by acoustic excitation. *Physics of Fluids*, 31(11):3260–3265, 1988.
- [4] H. Sakamoto and H. Haniu. A study on vortex shedding from spheres in an uniform flow. *Journal of Fluids Engineering*, 112:386–392, 1990.
- [5] Y.I Jang and S.J Lee. Visualization of turbulent flow around a sphere at subcritical Reynolds numbers. *Journal of Visualization*, 10(4):359–366, 2007.
- [6] V. Seidl, S. Muzaferija, and M. Peric. Parallel DNS with local grid refinement. *Applied Scientific Research*, 59:379–394, 1998.
- [7] A. Tomboulides and S.A. Orszag. Numerical investigation of transitional and weak turbulent flow past a sphere. *Journal of Fluids Mechanics*, 416:45–73, 2000.
- [8] P. Ploumhans, s G.S. Winckelman, J.K. Salmon, A. Leonard, and M.S. Warren. Vortex methods for a direct numerical simulation of three-dimensional bluff body flows: applications to the sphere at $re=300, 500$ and 1000 . *Journal of Computational Physics*, 178:427–463, 2002.
- [9] G. Constantinescu, M. Chapelet, and K. Squires. Turbulence modeling applied to flow over a sphere. *AIAA Journal*, 41(9):1733–1741, 2003.
- [10] R. Borrell, O. Lehmkuhl, F.X. Trias, M. Soria, and A. Oliva. Parallel direct poisson solver for dns of complex turbulent flows using unstructured meshes. In *Parallel Computational Fluid Dynamics*, Lyon, France, May 2008.
- [11] O. Lehmkuhl A. Oliva I. Rodríguez, R. Borrell and C.D. P èrez Segarra. Direct numerical simulation of the flow over a sphere at $re = 3700$. In *Turbulence, Heat and Mass Transfer, 2009*.
- [12] R. W. C. P. Verstappen and A. E. P. Veldman. Symmetry-Preserving Discretization of Turbulent Flow. *Journal of Computational Physics*, 187:343–368, May 2003.
- [13] G.M. Fishpool and M.A. Leschziner. Stability bounds for explicit fractional-step schemes for the Navier-Stokes equations at high Reynolds number. *Computers and Fluids*, 38:1289–1298, 2009.
- [14] C. M. Rhie and W. L. Chow. Numerical study of the turbulent flow past an airfoil with trailing edge separation. *AIAA Journal*, 21:1525–1532, 1983.
- [15] Y. Morinishi, T.S. Lund, O.V. Vasilyev, and P. Moin. Fully conservative higher order finite difference schemes for incompressible flow. *Journal of Computational Physics*, 143(1):90–124, 1998.

- [16] F.N. Felten and T.S. Lund. Kinetic energy conservation issues associated with the collocated mesh scheme for incompressible flow. *Journal of Computational Physics*, 215(2):465–484, 2006.
- [17] P.N. Swarztrauber. The Methods of Cyclic Reduction, Fourier Analysis and the FACR Algorithm for the Discrete Solution of Poisson’s Equation on a Rectangle. *SIAM Review*, 19:490–501, 1977.
- [18] M. Soria, C.D. Pérez-Segarra, and A. Oliva. A direct Schur-Fourier decomposition for the solution of three-dimensional Poisson equation of incompressible flow using loosely coupled parallel computers. *Numerical Heat Transfer, Part B*, 43(5):467–488, 2003.
- [19] Y. Saad and M. Sosenkina. Distributed Schur complement techniques for general sparse linear systems. *SIAM Journal of Scientific Computing*, 21(4):1337–1356, 1999.
- [20] J.C.R. Hunt, A.A. Wray, and P. Moin. Eddies, stream and convergence zones in turbulent flows. Technical Report CTR-S88, Center for turbulent research, 1988.
- [21] A.K. Norman and B.J. McKeon. Effect of the sting size in the wake of a sphere at subcritical reynolds numbers. In *38th Fluid Dynamics Conference and Exhibits, June 2008, Seattle, Washington*, volume AIAA 2008-4183, 2008.